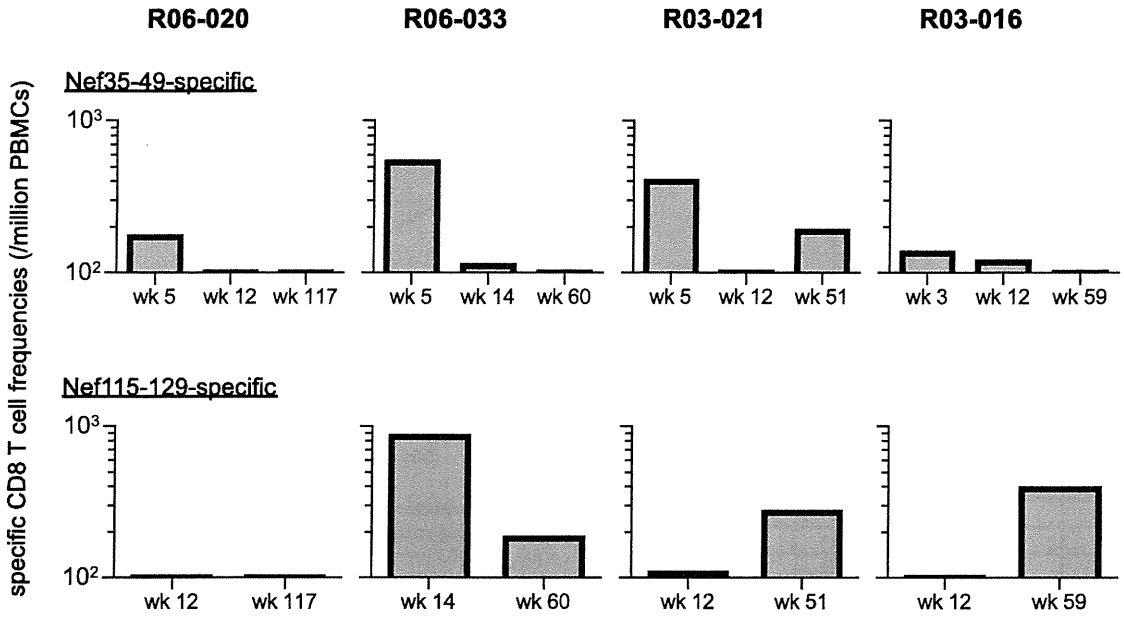

Figure 8. SIV Nef-specific CD8$^+$ T-cell responses in macaques R06-020, R06-033, R03-021, and R03-016. Nef_{35-49}-specific (upper panels) and $Nef_{115-129}$-specific (lower panels) CD8$^+$ T-cell responses were examined at indicated time points after SIVmac239 challenge.
doi:10.1371/journal.pone.0054300.g008

We then examined CD8$^+$ T-cell responses specific for individual SIV antigens in the early and the late phases (Fig. 3). Nef-specific but not Gag-specific CD8$^+$ T-cell responses were predominant in most D$^+$ animals. Gag-specific CD8$^+$ T-cell responses were dominantly induced in macaque R08-005 showing very low set-point viral loads. Macaque R01-012 having higher viral loads showed poor CD8$^+$ T-cell responses in the early phase.

Among four D$^+$ animals controlling SIV replication with less than 5×10^3 copies/ml of plasma viral loads after 6 months, Gag-specific CD8$^+$ T-cell responses were dominant only in macaque R08-005, while efficient Nef-specific CD8$^+$ T-cell responses were induced in the remaining three, suggesting possible contribution of Nef-specific CD8$^+$ T-cell responses to SIV control in these three controllers (R05-006, R06-034, and R-360). We then attempted to localize Nef CD8$^+$ T-cell epitopes shared in these animals and found Nef_{35-49}-specific and $Nef_{115-129}$-specific CD8$^+$ T-cell responses (Fig. 4), although we did not have enough samples for mapping the exact epitopes.

Reduction of Viral Loads in the Early Phase of SIV Infection by Prophylactic Vaccination

We also investigated SIVmac239 infection of additional five, vaccinated Burmese rhesus macaques sharing the MHC-I haplotype D. These animals received a prophylactic DNA/SeV-Gag vaccination. In four of these five vaccinated macaques, plasma viremia became undetectable after 6 months, while macaque R06-033 showed persistent viremia (Fig. 5A). Difference in viral loads between unvaccinated and vaccinated D$^+$ animals was unclear in the acute phase, but the latter vaccinees showed significant reduction in viral loads compared to those in the former unvaccinated at 3 months ($p = 0.0360$; Fig. 5B). After 6 months, unvaccinated animals also showed reduced viral loads, and the difference in viral loads between unvaccinated and vaccinated became unclear.

In contrast to unvaccinated D$^+$ animals, all five vaccinated animals elicited Gag-specific CD8$^+$ T-cell responses at week 2 after challenge (Fig. 6), reflecting the effect of prophylactic vaccination. We then examined CD8$^+$ T-cell responses specific for individual SIV antigens in these vaccinated animals (Fig. 7). Samples for this analysis were unavailable in vaccinated macaque R01-009. Vaccinated animals except for macaque R06-020 showed dominant Gag-specific CD8$^+$ T-cell responses even at 1–2 months. However, Gag-specific CD8$^+$ T-cell responses became not dominant after 1 year, while Nef-specific or Vif-specific CD8$^+$ T-cell responses became predominant, instead, in most vaccinees except for macaque R03-016.

Like three unvaccinated macaques (R05-006, R06-034, and R-360), vaccinated D$^+$ animals induced Nef_{35-49}-specific and $Nef_{115-129}$-specific CD8$^+$ T-cell responses after SIV challenge (Fig. 8). In analyses of three unvaccinated (Fig. 4) and four vaccinated animals (Fig. 8), Nef_{35-49}-specific CD8$^+$ T-cell responses were induced in the early phase in six animals but mostly became undetectable in the chronic phase. $Nef_{115-129}$-specific CD8$^+$ T-cell responses were also induced in most animals except for macaque R06-020 which showed $Nef_{112-126}$-specific ones in the chronic phase (data not shown). Macaques R05-006, R03-021, and R03-016 showed efficient $Nef_{115-129}$-specific CD8$^+$ T-cell responses not in the early phase but in the chronic phase. In contrast, vaccinated animal R06-033 that failed to control viremia showed higher $Nef_{115-129}$-specific CD8$^+$ T-cell responses in the early phase than those in the chronic phase.

Selection of Mutations in Nef CD8$^+$ T-cell Epitope-coding Regions

To see the effect of selective pressure by Nef-specific CD8$^+$ T-cell responses on viral genome mutations, we next analyzed nucleotide sequences in viral *nef* cDNAs amplified from plasma RNAs obtained at several time points after SIV challenge. Nonsynonymous mutations detected predominantly in Nef_{35-49}-coding and $Nef_{115-129}$-coding regions were as shown in Fig. 9. Remarkably, all the unvaccinated and vaccinated D$^+$ animals showed rapid selection of mutations in the Nef_{35-49}-coding region in 3 months. On the other hand, mutations in the $Nef_{115-129}$-coding region were observed in the late phase in all the three

		Nef35-49						Nef115-129				
Nef		36	37	41	42	44		119	122	124	125	126
		E	D	Q	S	G		M	F	K	E	K
R01-012	1M		*G									
	3M		*G									
	14M	*G	*G									
	24M	*G	*G			*E						
R05-006	1M					*E						
	3M			R								
	16M			R								
	24M			R								R
R06-034	1M											
	3M	*G										
	10M	*G	*G			*E						*R
	18M	G				E						R
R08-005	1M											
	3M				*F							
	6M	G										
	14M				F							
	24M	*G			F							
R-360	1M											
	3M		*G									
	6M		G									
	12M		G					T	L			
	20M		G					T	L			
R06-020	1M											
	3M	*K										
	11M		G	R								
R06-033	1M											
	3M	*G										
	6M		*G									
	14M		G			*E					K	E
R03-021	1M											
	3M				*F							
	14M	G								R		
R03-016	1M	*K		*R								
	4M	K										
	12M	K										

Figure 9. Predominant non-synonymous mutations in Nef_{35-49}-coding and $Nef_{115-129}$-coding regions of viral cDNAs in D^+ animals after SIVmac239 challenge. Amino acid substitutions are shown. Detection of similar levels of wild-type and mutant sequences at the residue is indicated by asterisks. Samples for this analysis were unavailable in macaque R01-009.
doi:10.1371/journal.pone.0054300.g009

unvaccinated animals eliciting $Nef_{115-129}$-specific $CD8^+$ T-cell responses. These mutations were also detected in two of three vaccinated animals eliciting $Nef_{115-129}$-specific $CD8^+$ T-cell responses.

We also analyzed viral *gag* sequences to see the effect of Gag-specific $CD8^+$ T-cell pressure on viral genome mutations in vaccinated animals (data not shown). Our previous study [35] showed rapid selection of a mutation leading to a glutamine (Q)-to-lysine (K) change at the 58th residue in Gag (Q58K) at week 5 in vaccinated macaque R01-009, although no more samples were available for this sequencing analysis. This Q58K mutation results in escape from Gag_{50-65}-specific $CD8^+$ T-cell recognition. In the present study, macaque R03-016 showed rapid selection of a mutation leading to a K-to-asparagine (N) change at the 478th residue in Gag in 1 month. These results may reflect rapid disappearance of detectable plasma viremia in 1 or 2 months in these two vaccinees. Macaque R06-020 showed selection of a *gag* mutation in 3 months, while other two vaccinees (R06-033 and R03-021) selected no *gag* mutation in the early phase.

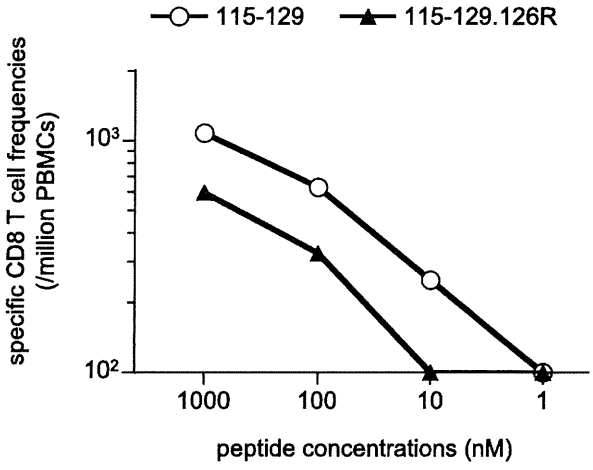

Figure 10. IFN-γ induction in $CD8^+$ T cells after stimulation with the wild-type or the mutant peptide. PBMCs obtained at week 31 from macaque R06-033 were stimulated by coculture with B-LCL pulsed with indicated concentrations of the wild-type $Nef_{115-129}$ peptide (open circles, 115–129, LAIDMSHFIKEKGGL) or the mutant $Nef_{115-129}$ peptide with a K126R alteration (closed triangles, 115–129.126R, LAIDMSHFIKERGGL).
doi:10.1371/journal.pone.0054300.g010

Discussion

HIV infection in humans with polymorphic MHC-I genotypes induces various patterns of viral antigen-specific $CD8^+$ T-cell responses. Previous studies have found several protective MHC-I alleles associated with lower viral loads and slower disease progression in HIV/SIV infection [7,13,14,16,17]. Elucidation of the mechanisms of viral control associated with individual protective MHC-I alleles would contribute to HIV cure and vaccine-based prevention. Because $CD8^+$ T-cell responses specific for some MHC-I-restricted epitopes can be affected by those specific for other MHC-I-restricted epitopes due to immunodominance [29,46,47], macaque groups sharing MHC-I genotypes at the haplotype level are useful for the analysis of cooperation of multiple epitope-specific $CD8^+$ T-cell responses. Previously, we reported a group of Burmese rhesus macaques sharing MHC-I haplotype *90-120-Ia* (A), which dominantly induce Gag-specific $CD8^+$ T-cell responses and tend to show slower disease progression after SIVmac239 challenge [21]. In the present study, we presented another type of protective MHC-I haplotype, which is not associated with dominant Gag-specific $CD8^+$ T-cell responses. Significant reduction of viral loads in unvaccinated macaques possessing this D haplotype compared to those in D^- macaques was observed after 6 months. Analysis of SIV infection in macaques sharing this protective MHC-I haplotype would lead to understanding of $CD8^+$ T-cell cooperation for viral control.

Analyses of antigen-specific $CD8^+$ T-cell responses after SIVmac239 challenge indicate that this MHC-I haplotype D is associated with predominant Nef-specific $CD8^+$ T-cell responses. Nef-specific $CD8^+$ T-cell responses were efficiently induced in all SIV controllers, whereas Gag-specific $CD8^+$ T-cell responses were dominant in only one of them. We found Nef_{35-49}-specific and $Nef_{115-129}$-specific $CD8^+$ T-cell responses shared in D^+ animals. We were unable to determine the MHC-I alleles restricting these epitopes, but these responses are not usually induced in our

previous D^- cohorts and considered to be associated with this MHC-I haplotype D.

Sequencing analysis of viral genomes showed rapid selection of mutations in the Nef_{36-44}-coding region within 3 months in all the D^+ animals. This is consistent with our results that Nef_{35-49}-specific $CD8^+$ T-cell responses were mostly induced in the early phase but undetectable in the chronic phase. These mutations were not consistently selected in our previous D^- cohorts and thus considered as MHC-I haplotype D-associated mutations. This suggests strong selective pressure by Nef_{35-49}-specific $CD8^+$ T-cell responses in the acute phase of SIVmac239 infection in D^+ macaques, although it remains undetermined whether these mutations result in viral escape from Nef_{35-49}-specific $CD8^+$ T-cell recognition.

$Nef_{115-129}$-specific $CD8^+$ T-cell responses were detected in six D^+ animals. In five of them, nonsynonymous mutations in the $Nef_{119-126}$-coding region were observed in the chronic phase. At least, we confirmed viral escape from $Nef_{115-129}$-specific $CD8^+$ T-cell recognition by a mutation leading to a K-to-arginine (R) (K126R) substitution at Nef residue 126 (Fig. 10). The number of nonsynonymous substitutions per the number of sites estimated to be nonsynonymous (dN) exceeded that estimated to be synonymous (dS) during the evolution process of $Nef_{115-129}$-coding region, but the value did not show statistically significant difference from that of neutral selection. Among three unvaccinated animals that controlled SIV replication without dominant Gag-specific $CD8^+$ T-cell responses, amino acid substitutions in the $Nef_{119-126}$-coding region were observed in a year in macaques R06-034 and R-360 but after 2 years in macaque R05-006. The former two animals tended to show earlier increases in plasma viral loads in the chronic phase, while the latter R05-006 maintained higher frequencies of $Nef_{115-129}$-specific $CD8^+$ T-cell responses. $Nef_{115-129}$-specific $CD8^+$ T-cell responses were efficient in the chronic phase in vaccinated controllers R03-021 and R03-016 but decreased in R06-033 that failed to contain SIV replication. Although a possible effect of this haplotype-associated factors other than $CD8^+$ T-cell responses such as NK activity on SIV infection [48,49,50] remains undetermined, these results imply involvement of Nef-specific $CD8^+$ T-cell responses in the SIV control associated with MHC-I haplotype D.

Unvaccinated macaque R08-005 dominantly elicited Gag antigen-specific $CD8^+$ T-cell responses and showed rapid selection of a mutation encoding Gag 257 residue, which was not observed in any other D^+ animals. Nef-specific $CD8^+$ T-cell responses were detectable only at week 2 in the acute phase (data not shown) and a mutation in the Nef_{42}-coding region was rapidly selected. It is speculated that those dominant Gag-specific $CD8^+$ T-cell responses associated with the second, non-D MHC-I haplotype were effective in this animal. Nef_{35-49}-specific $CD8^+$ T-cell responses may not be efficient due to immunodominance but exert some suppressive pressure on viral replication.

DNA/SeV-Gag vaccination resulted in earlier reduction of viral loads after SIV challenge. Vaccinees showed significantly lower viral loads at 3 months than those in unvaccinated animals. Gag-specific $CD8^+$ T-cell responses were elicited at week 2 in all the vaccinees but not in the unvaccinated except for one animal R08-005. No *gag* mutations were shared in the vaccinees in the acute phase, but three of them showed rapid selection of individual non-synonymous mutations in *gag*. Rapid selection of mutations in the Nef_{36-44}-coding region was consistently detected even in these vaccinees. These results suggest broader $CD8^+$ T-cell responses consisting of dominant vaccine antigen Gag-specific and inefficient naive-derived Nef-specific ones in the acute phase. In three vaccinated animals, Gag-specific $CD8^+$ T-cell responses became lower or undetectable, and instead, Nef-specific $CD8^+$ T-cell responses became predominant in the chronic phase.

In summary, we found a protective MHC-I haplotype not associated with dominant Gag-specific $CD8^+$ T-cell responses in SIVmac239 infection. Our results in D^+ macaques suggest suppressive pressure by Nef_{35-49}-specific and $Nef_{115-129}$-specific $CD8^+$ T-cell responses on SIV replication, contributing to reduction in set-point viral loads. DNA/SeV-Gag-vaccinated D^+ animals induced Gag-specific $CD8^+$ T-cell responses in addition to Nef-specific ones after SIV challenge, resulting in earlier containment of SIV replication. This study presents a pattern of SIV control with involvement of non-Gag antigen-specific $CD8^+$ T-cell responses, contributing to accumulation of our knowledge on HIV/SIV control mechanisms.

Acknowledgments

We thank F. Ono, K. Oto, K. Hanari, K. Komatsuzaki, M. Hamano, H. Akari, and Y. Yasutomi for their assistance in animal experiments.

Author Contributions

Performed animal experiments: HS TM TI YK. Performed MHC-I typing: TKN AK. Conceived and designed the experiments: NT TM. Performed the experiments: NT TN YT HY AT. Analyzed the data: NT HY T. Shiino TM. Contributed reagents/materials/analysis tools: MI AI HH T. Shu MH. Wrote the paper: NT TM.

References

1. Borrow P, Lewicki H, Hahn BH, Shaw GM, Oldstone MB (1994) Virus-specific CD8+ cytotoxic T-lymphocyte activity associated with control of viremia in primary human immunodeficiency virus type 1 infection. J Virol 68: 6103–6110.
2. Koup RA, Safrit JT, Cao Y, Andrews CA, McLeod G, et al. (1994) Temporal association of cellular immune responses with the initial control of viremia in primary human immunodeficiency virus type 1 syndrome. J Virol 68: 4650–4655.
3. Matano T, Shibata R, Siemon C, Connors M, Lane HC, et al. (1998) Administration of an anti-CD8 monoclonal antibody interferes with the clearance of chimeric simian/human immunodeficiency virus during primary infections of rhesus macaques. J Virol 72: 164–169.
4. Jin X, Bauer DE, Tuttleton SE, Lewin S, Gettie A, et al. (1999) Dramatic rise in plasma viremia after CD8+ T cell depletion in simian immunodeficiency virus-infected macaques. J Exp Med 189: 991–998.
5. Schmitz JE, Kuroda MJ, Santra S, Sasseville VG, Simon MA, et al. (1999) Control of viremia in simian immunodeficiency virus infection by CD8+ lymphocytes. Science 283: 857–860.
6. Carrington M, Nelson GW, Martin MP, Kissner T, Vlahov D, et al. (1999) HLA and HIV-1: heterozygote advantage and B*35-Cw*04 disadvantage. Science 283: 1748–1752.
7. Migueles SA, Sabbaghian MS, Shupert WL, Bettinotti MP, Marincola FM, et al. (2000) HLA B*5701 is highly associated with restriction of virus replication in a subgroup of HIV-infected long term nonprogressors. Proc Natl Acad Sci USA 97: 2709–2714.
8. Tang J, Tang S, Lobashevsky E, Myracle AD, Fideli U, et al. (2002) Favorable and unfavorable HLA class I alleles and haplotypes in Zambians predominantly infected with clade C human im- munodeficiency virus type 1. J Virol 76: 8276–8284.
9. Kiepiela P, Leslie AJ, Honeyborne I, Ramduth D, Thobakgale C, et al. (2004) Dominant influence of HLA-B in mediating the potential co-evolution of HIV and HLA. Nature 432: 769–775.
10. Leslie A, Matthews PC, Listgarten J, Carlson JM, Kadie C, et al. (2010) Additive contribution of HLA class I alleles in the immune control of HIV-1 infection. J Virol 84: 9879–9888.
11. Altfeld M, Addo MM, Rosenberg ES, Hecht FM, Lee PK, et al. (2003) Influence of HLA-B57 on clinical presentation and viral control during acute HIV-1 infection. AIDS 17: 2581–2591.
12. Altfeld M, Kalife ET, Qi Y, Streeck H, Lichterfeld M, et al. (2006) HLA alleles associated with delayed progression to AIDS contribute strongly to the initial CD8+ T cell response against HIV-1. PLoS Med 3: e403.
13. Goulder PJ, Watkins DI (2008) Impact of MHC class I diversity on immune control of immunodeficiency virus replication. Nat Rev Immunol 8: 619–630.

14. Muhl T, Krawczak M, Ten Haaft P, Hunsmann G, Sauermann U (2002) MHC class I alleles influence set-point viral load and survival time in simian immunodeficiency virus-infected rhesus monkeys. J Immunol 169: 3438–3446.
15. Mothe BR, Weinfurter J, Wang C, Rehrauer W, Wilson N, et al. (2003) Expression of the major histocompatibility complex class I molecule Mamu-A*01 is associated with control of simian immunodeficiency virus SIVmac239 replication. J Virol 77: 2736–2740.
16. Yant LJ, Friedrich TC, Johnson RC, May GE, Maness NJ, et al. (2006) The high-frequency major histocompatibility complex class I allele Mamu-B*17 is associated with control of simian immunodeficiency virus SIVmac239 replication. J Virol 80: 5074–5077.
17. Loffredo JT, Maxwell J, Qi Y, Glidden CE, Borchardt GJ, et al. (2007) Mamu-B*08-positive macaques control simian immunodeficiency virus replication. J Virol 81: 8827–8832.
18. Edwards BH, Bansal A, Sabbaj S, Bakari J, Mulligan MJ, et al. (2002) Magnitude of functional CD8+ T-cell responses to the gag protein of human immunodeficiency virus type 1 correlates inversely with viral load in plasma. J Virol 76: 2298–2305.
19. Zuniga R, Lucchetti A, Galvan P, Sanchez S, Sanchez C, et al. (2006) Relative dominance of Gag p24-specific cytotoxic T lymphocytes is associated with human immunodeficiency virus control. J Virol 80: 3122–3125.
20. Kiepiela P, Ngumbela K, Thobakgale C, Ramduth D, Honeyborne I, et al. (2007) CD8+ T-cell responses to different HIV proteins have discordant associations with viral load. Nat Med 13: 46–53.
21. Nomura T, Yamamoto H, Shiino T, Takahashi N, Nakane T, et al. (2012) Association of major histocompatibility complex class I haplotypes with disease progression after simian immunodeficiency virus challenge in Burmese rhesus macaques. J Virol 86: 6481–6490.
22. Schneidewind A, Brockman MA, Yang R, Adam RI, Li B, et al. (2007) Escape from the dominant HLA-B27-restricted cytotoxic T-lymphocyte response in Gag is associated with a dramatic reduction in human immunodeficiency virus type 1 replication. J Virol 81: 12382–12393.
23. Emu B, Sinclair E, Hatano H, Ferre A, Shacklett B, et al. (2008) HLA class I-restricted T-cell responses may contribute to the control of human immunodeficiency virus infection, but such responses are not always necessary for long-term virus control. J Virol 82: 5398–5407.
24. Miura T, Brockman MA, Schneidewind A, Lobritz M, Pereyra F, et al. (2009) HLA-B57/B*5801 human immunodeficiency virus type 1 elite controllers select for rare gag variants associated with reduced viral replication capacity and strong cytotoxic T-lymphocyte recognition. J Virol 83: 2743–2755.
25. Leslie AJ, Pfafferott KJ, Chetty P, Draenert R, Addo MM, et al. (2004) HIV evolution: CTL escape mutation and reversion after transmission. Nat Med 10: 282–289.
26. Martinez-Picado J, Prado JG, Fry EE, Pfafferott K, Leslie A, et al. (2006) Fitness cost of escape mutations in p24 Gag in association with control of human immunodeficiency virus type 1. J Virol 80: 3617–3623.
27. Crawford H, Prado JG, Leslie A, Hue S, Honeyborne I, et al. (2007) Compensatory mutation partially restores fitness and delays reversion of escape mutation within the immunodominant HLA-B*5703-restricted Gag epitope in chronic human immunodeficiency virus type 1 infection. J Virol 81: 8346–8351.
28. Friedrich TC, Valentine LE, Yant LJ, Rakasz EG, Piaskowski SM, et al. (2007) Subdominant CD8+ T-cell responses are involved in durable control of AIDS virus replication. J Virol 81: 3465–3476.
29. Loffredo JT, Bean AT, Beal DR, Leon EJ, May GE, et al. (2008) Patterns of CD8+ immunodominance may influence the ability of Mamu-B*08-positive macaques to naturally control simian immunodeficiency virus SIVmac239 replication. J Virol 82: 1723–1738.
30. Maness NJ, Yant LJ, Chung C, Loffredo JT, Friedrich TC, et al. (2008) Comprehensive immunological evaluation reveals surprisingly few differences between elite controller and progressor Mamu-B*17-positive simian immunodeficiency virus-infected rhesus macaques. J Virol 82: 5245–5254.
31. Valentine LE, Loffredo JT, Bean AT, Leon EJ, MacNair CE, et al. (2009) Infection with "escaped" virus variants impairs control of simian immunodeficiency virus SIVmac239 replication in Mamu-B*08-positive macaques. J Virol 83: 11514–11527.
32. Budde ML, Greene JM, Chin EN, Ericsen AJ, Scarlotta M, et al. (2012) Specific CD8+ T cell responses correlate with control of simian immunodeficiency virus replication in Mauritian cynomolgus macaques. J Virol 86: 7596–7604.
33. Mudd PA, Martins MA, Ericsen AJ, Tully DC, Power KA, et al. (2012) Vaccine-induced CD8+ T cells control AIDS virus replication. Nature 491: 129–133.
34. Naruse TK, Chen Z, Yanagida R, Yamashita T, Saito Y, et al. (2010) Diversity of MHC class I genes in Burmese-origin rhesus macaques. Immunogenetics 62: 601–611.
35. Matano T, Kobayashi M, Igarashi H, Takeda A, Nakamura H, et al. (2004) Cytotoxic T lymphocyte-based control of simian immunodeficiency virus replication in a preclinical AIDS vaccine trial. J Exp Med 199: 1709–1718.
36. Kawada M, Tsukamoto T, Yamamoto H, Iwamoto N, Kurihara K, et al. (2008) Gag-specific cytotoxic T-lymphocyte-based control of primary simian immunodeficiency virus replication in a vaccine trial. J Virol 82: 10199–10206.
37. Tanaka-Takahashi Y, Yasunami M, Naruse T, Hinohara K, Matano T, et al. (2007) Reference strand-mediated conformation analysis-based typing of multiple alleles in the rhesus macaque MHC class I Mamu-A and Mamu-B loci. Electrophoresis 28: 918–924.
38. Shibata R, Maldarelli F, Siemon C, Matano T, Parta M, et al. (1997) Infection and pathogenicity of chimeric simian-human immunodeficiency viruses in macaques: determinants of high virus loads and CD4 cell killing. J Infect Dis 176: 362–373.
39. Li HO, Zhu YF, Asakawa M, Kuma H, Hirata T, et al. (2000) A cytoplasmic RNA vector derived from nontransmissible Sendai virus with efficient gene transfer and expression. J Virol 74: 6564–6569.
40. Takeda A, Igarashi H, Nakamura H, Kano M, Iida A, et al. (2003) Protective efficacy of an AIDS vaccine, a single DNA priming followed by a single booster with a recombinant replication-defective Sendai virus vector, in a macaque AIDS model. J Virol 77: 9710–9715.
41. Kestler HW III, Ringler DJ, Mori K, Panicali DL, Sehgal PK, et al. (1991) Importance of the nef gene for maintenance of high virus loads and for development of AIDS. Cell 65: 651–662.
42. Yamamoto H, Kawada M, Takeda A, Igarashi H, Matano T (2007) Post-infection immunodeficiency virus control by neutralizing antibodies. PLoS One 2: e540.
43. Iwamoto N, Tsukamoto T, Kawada M, Takeda A, Yamamoto H, et al. (2010) Broadening of CD8+ cell responses in vaccine-based simian immunodeficiency virus controllers. AIDS 24: 2777–2787.
44. Voss G, Nick S, Stahl-Hennig C, Ritter K, Hunsmann G (1992) Generation of macaque B lymphoblastoid cell lines with simian Epstein-Barr-like viruses: transformation procedure, characterization of the cell lines and occurrence of simian foamy virus. J Virol Methods 39: 185–195.
45. Kawada M, Igarashi H, Takeda A, Tsukamoto T, Yamamoto H, et al. (2006) Involvement of multiple epitope-specific cytotoxic T-lymphocyte responses in vaccine-based control of simian immunodeficiency virus replication in rhesus macaques. J Virol 80: 1949–1958.
46. Tenzer S, Wee E, Burgevin A, Stewart-Jones G, Friis L, et al. (2009) Antigen processing influences HIV-specific cytotoxic T lymphocyte immunodominance. Nat Immunol 10: 636–646.
47. Ishii H, Kawada M, Tsukamoto T, Yamamoto H, Matsuoka S, et al. (2012) Impact of vaccination on cytotoxic T lymphocyte immunodominance and cooperation against simian immunodeficiency virus replication in rhesus macaques. J Virol 86: 738–745.
48. Flores-Villanueva PO, Yunis EJ, Delgado JC, Vittinghoff E, Buchbinder S, et al. (2001) Control of HIV-1 viremia and protection from AIDS are associated with HLA-Bw4 homozygosity. Proc Natl Acad Sci USA 98: 5140–5145.
49. Martin MP, Gao X, Lee JH, Nelson GW, Detels R, et al. (2002) Epistatic interaction between KIR3DS1 and HLA-B delays the progression to AIDS. Nat Genet 31: 429–434.
50. Martin MP, Qi Y, Gao X, Yamada E, Martin JN, et al. (2007) Innate partnership of HLA-B and KIR3DL1 subtypes against HIV-1. Nat Genet 39: 733–740.

JVI
Journals.ASM.org

No Viral Evolution in the Lymph Nodes of Simian Immunodeficiency Virus-Infected Rhesus Macaques during Combined Antiretroviral Therapy

Megu Oue, Saori Sakabe, Mariko Horiike, Mika Yasui, Tomoyuki Miura, Tatsuhiko Igarashi

Laboratory of Primate Model, Experimental Research Center for Infectious Diseases, Institute for Virus Research, Kyoto University, Kyoto, Japan

To elucidate the mode of viral persistence in primate lentivirus-infected individuals during combination antiretroviral therapy (cART), four simian immunodeficiency virus 239-infected monkeys were treated with cART for 1 year. The viral *env* genes prepared from total RNA extracted from the mesenteric lymph nodes collected at the completion of therapy were assessed by single genome amplification. Analyses of nucleotide substitutions and phylogeny revealed no viral evolution during cART.

Combination antiretroviral therapy (cART) has transformed human immunodeficiency virus (HIV) infection from an incurable disease to a manageable one. It suppresses the viral burden in patients to undetectable levels (1–3), lowers the chance of viral transmission (4), increases the number of $CD4^+$ T lymphocytes (1, 2), reconstitutes immunity (5–7), and extends the life expectancy of patients (8). However, cART does not cure patients because of its inability to eradicate the virus from infected individuals (9), suggesting the existence of a viral reservoir that is refractory to cART. Its identification and eradication are therefore requisites for a functional cure for AIDS. To establish a strategy for eradication of the HIV reservoir, the mechanism of persistence of the virus must be elucidated. Two mechanisms of viral persistence have been proposed: one is ongoing cycles of viral replication despite the presence of antivirals (10), and the other is provirus integration into long-lived cells (11). Whereas previous studies concerning this issue have been extensively conducted with clinical specimens from HIV-1-infected patients, including plasma, peripheral blood mononuclear cells, and gut-associated lymphatic tissues (12–14), lymph nodes, which are epicenters of virus replication in infected individuals not undergoing therapy (15–17), have only rarely been subjected to scrutiny. In animal models of cART, in particular, the simian immunodeficiency virus (SIV)-macaque model, which allows systemic examination, the location of the viral reservoir and the mechanism of viral holding have not been studied in detail.

To elucidate how the virus is maintained during cART in an animal model of anti-HIV chemotherapy, we administered a combination of nucleotide/nucleoside reverse transcriptase inhibitors (azidothymidine, lamivudine, and tenofovir disoproxil fumarate) and protease inhibitors (lopinavir with ritonavir) to four SIV239-infected rhesus macaques for 1 year (18). Although the plasma viral RNA loads of the animals were suppressed to levels below the assay detection limit during the period of chemotherapy, a systemic analysis conducted at the completion of therapy revealed viral RNA present in lymphatic tissues, especially in mesenteric and splenic lymph nodes (MLN and SLN, respectively) at high titers. Reasoning that any possible mode(s) of viral persistence should be in operation in tissues with high levels of viral RNA expression, we investigated viral genes in these tissues.

It is expected that viral genes accumulate nucleotide substitutions in proportion to the time postinfection in individuals not undergoing therapy because of continuous virus replication mediated by the error-prone viral reverse transcriptase. Such mutation rates have indeed been observed in the V3 loop of *env*, p17 of *gag* (19), and the C2-to-C5 region of *env* (20) in HIV-1-infected patients, as well as in the *env* gene from monkeys experimentally infected with SIV (21, 22). We hypothesized that viral genes would accumulate mutations if the virus was continuously replicating in the reservoir despite the presence of antivirals.

First, to ascertain whether such an accumulation of mutations took place at a detectable magnitude in our experimental system, we used SIV239, a molecularly cloned virus, to infect macaques for 1 year and periodically sampled viral genes from the untreated control animal (MM521). To reveal ongoing expression of viral genes at sampling, total RNA was extracted from plasma samples collected at 8, 18, 42, and 68 weeks postinfection (wpi) and examined. Single-genome amplification (SGA) (23) was used to amplify the viral genes present and to avoid the selective amplification of a particular genotype or recombination between genotypes during PCR. Using a nested PCR method, we amplified the entire *env* gene, which accumulates nucleotide substitutions in the greatest numbers, following reverse transcription of cDNA from the extracted RNA. The initial PCR cycles were carried out with the following primers: forward, SIV20F (5′-CTC CAG GAC TAG CAT AAA TGG-3′); reverse, SHenv9R (5′-GGG TAT CTA ACA TAT GCC TC-3′). Successive PCR cycles were run with the following primers: forward, SIV21F (5′-CTC TCT CAG CTA TAC CGC CC-3′); reverse, SHenv8R (5′-GCC TTC TTC CTT TTC TAA G-3′). The PCR products from an average of 12 independent reactions per time point were directly subjected to sequencing.

We computed the number of mutations in each SGA clone obtained from plasma samples of an untreated monkey (MM521) through a comparison with that of the inoculum virus (Fig. 1). A

Received 6 December 2012 Accepted 2 February 2013
Published ahead of print 13 February 2013
Address correspondence to Tatsuhiko Igarashi, tigarash@virus.kyoto-u.ac.jp.
Supplemental material for this article may be found at http://dx.doi.org/10.1128/JVI.03367-12.

doi:10.1128/JVI.03367-12

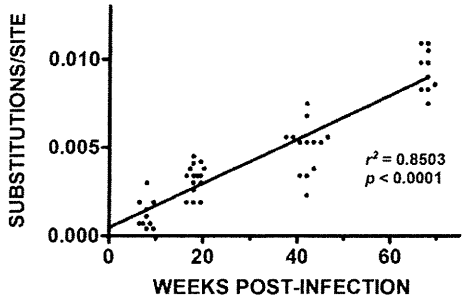

FIG 1 Time-dependent accumulation of nucleotide substitutions in SIV genomes circulating in an infected and untreated rhesus macaque. The sequences of viral *env* genes in circulation collected at 8, 18, 42, and 68 wpi from SIV239-infected animals and an untreated animal (MM521) were determined. Tamura-Nei distances (36) of the sequences were computed with the MEGA5 software (37), and the number of nucleotide substitutions per site was plotted against the number of weeks postinfection. Each symbol represents a single genomic amplicon derived from plasma samples collected at the time points designated.

linear relationship with a coefficient of 1.25×10^{-4} ($r^2 = 0.8503$, $P < 0.0001$; GraphPad Prism, La Jolla, CA) was revealed between the number of mutations in the SGA clones and the time postinfection. By using the coefficient, the cumulative number of mutations per annum was determined to be 6.5×10^{-3} substitutions/site/year, a value comparable to those of SIV and HIV reported previously (9×10^{-3} [21, 22] and 6.0×10^{-3} [23] substitutions/site/year, respectively). The accuracy of the "molecular clock" in our experimental setting prompted us to examine viral RNA extracted from the lymph nodes of animals that underwent cART for 1 year.

Total RNA was extracted from the MLN of four treated animals and one untreated animal, as well as the SLN of one of the treated animals (MM530), at the completion of the observation period and used as the template for PCR; the products were subjected to sequence analysis as described above. On average, 10 sequences were obtained from each sample (Fig. 2A and Table 1). The number of mutations observed in the *env* gene from MM521 (untreated) was, on average, 25 of 2,700 bases. In contrast, the number in treated animals was, on average, 1.5 of 2,700 bases (Table 1). The difference in the number of mutations in *env* between the plasma and MLN samples from the untreated animal, MM521, at 68 wpi (at necropsy) was statistically insignificant ($P > 0.05$; Fig. 2A), justifying our comparison of these two distinct anatomical compartments. Thus, we proceeded to compare the substitution numbers in plasma at 8 wpi, immediately before the onset of cART, with those from the lymph nodes of animals treated with cART at necropsy (61 to 65 wpi). The number of nucleotide substitutions in the *env* gene in both the plasma and MLN of the untreated animal (MM521) at 68 wpi was higher than that in plasma at 8 wpi ($P < 0.0001$). In contrast, those in the MLN of treated animals at the completion of cART were unchanged (MM528 and SLN of MM530) or decreased significantly (MM491, MM499, and MLN of MM530) (Fig. 2A). The results indicated that the virus did not accumulate further mutations beyond those obtained by 8 wpi.

As the samples were collected from animals at various time points postinfection, the numbers depicted in Fig. 2A were converted to substitutions/site/year (Fig. 2B) for further analysis. Comparison of the number of viral mutations in plasma at 8 wpi

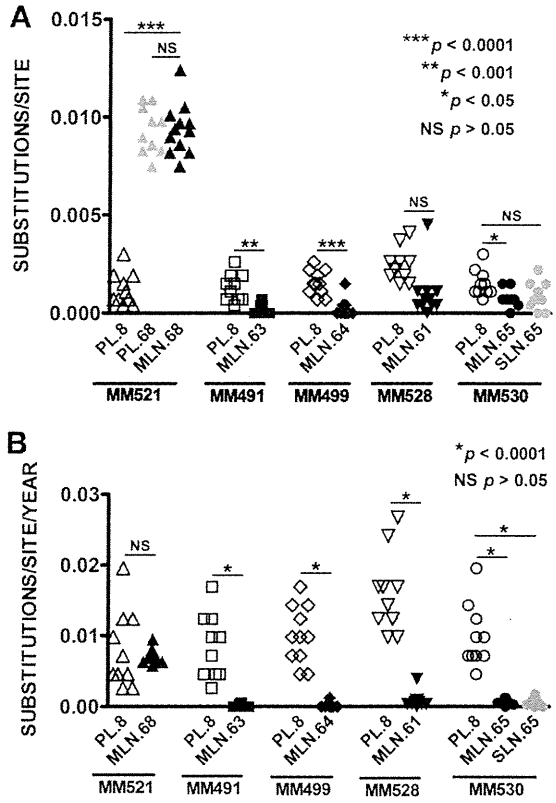

FIG 2 Nucleotide substitutions in *env* genes from SIV239-infected animals. The number of mutations in *env* from the plasma (PL, at 8 and 68 wpi) and MLN (at 68 wpi) of an SIV-infected but untreated animal (MM521) and from the plasma (at 8 wpi) and MLN (at necropsy, 61, 63, 64, or 65 wpi) and SLN (at necropsy, 65 wpi) from SIV-infected and treated monkeys (MM491, MM499, MM528, and MM530) were assessed as described in the legend to Fig. 1. (A) Numbers of nucleotide substitutions per site are shown. The statistical significance of differences between substitution numbers was evaluated by Student's *t* test using GraphPad Prism. *, $P < 0.05$; **, $P < 0.001$; ***, $P < 0.0001$; NS, $P > 0.05$. (B) Numbers of nucleotide substitutions per annum are shown. *, $P < 0.001$; NS, $P > 0.05$.

(median, 5.9×10^{-3} substitutions/site/year) with that in the MLN (median, 7.2×10^{-3} substitutions/site/year) in the untreated animal, MM521, indicated no statistically significant difference ($P = 0.6265$), as predicted by the analysis in Fig. 2A. Next, we compared the numbers in animals that underwent chemotherapy. At 8 wpi, the treated animals were equivalent to MM521 (an untreated animal) in terms of therapeutic status, since cART was started after sample collection at 8 wpi. Not unexpectedly, there was no statistically significant difference in the number of substitutions/site/year in plasma between the untreated and treated animals (MM491, 8.5×10^{-3}; MM499, 9.8×10^{-3}; MM528, 1.6×10^{-2}; MM530, 8.5×10^{-3}; MM521, 5.9×10^{-3}), except for MM528 ($P = 0.0048$ compared to the value for the untreated animal). In contrast, the number of mutations per annum in the lymph nodes of treated animals collected at necropsy (median, 3.4×10^{-4} substitutions/site/year) was significantly lower than that in the plasma of the animals at 8 wpi (median, 9.8×10^{-3} substitutions/site/year; $P < 0.0001$). The number of mutations per year in the lymph nodes also differed significantly between the untreated and treated macaques ($P < 0.0001$). This supports the hypothesis that ongoing viral replication contributed little, if anything, to viral persistence during cART.

TABLE 1 Origins and numbers of *env* clones

Animal (cART) and specimen	Sample collection time (wpi)	No. of SGA clones	No. of nucleotide substitutions	
			Minimum/ maximum	Mean ± SD
MM521 (untreated)				
Plasma	8	10	1/8	3.3 ± 2.2
Plasma	68	10	20/29	24.9 ± 3.2
MLN	68	12	20/33	25.0 ± 3.4
MM491 (treated)				
Plasma	8	10	1/7	3.5 ± 1.8
MLN	63	10	0/2	0.6 ± 0.8
MM499 (treated)				
Plasma	8	11	2/7	4.2 ± 1.7
MLN	64	10	0/4	0.7 ± 1.3
MM528 (treated)				
Plasma	8	10	4/11	6.6 ± 2.4
MLN	61	11	0/3 (12)[a]	1.7 ± 1.1[b]
MM530 (treated)				
Plasma	8	10	2/8	4.0 ± 1.7
MLN	65	10	0/4	2.1 ± 1.2
SLN	65	10	0/6	2.4 ± 1.9

[a] Interpreted as a hypermutant driven by APOBEC3G/F (Hypermut 2.0, http://www.hiv.lanl.gov/content/index).
[b] Computed excluding the clone with hypermutation.

Examination of the nucleotide substitution numbers did not indicate discernible *de novo* virus replication during cART. Therefore, we next investigated continuous viral replication during cART through phylogenetic analysis of viral *env* clones. Clones were obtained from the untreated animal (derived from plasma at 8, 18, 42, and 68 wpi and from MLN) and from one of the treated animals (derived from plasma at 8 wpi and from MLN at necropsy) (Fig. 3; see Fig. S1 in the supplemental material). To illustrate the accumulation and specific sites of mutations, Highlighter plot analysis (http://www.hiv.lanl.gov/content/sequence/HIGHLIGHT/help.html) was also performed. Phylogenetic analysis of the viral genes from the untreated animal revealed that (i) *env* clones from plasma exhibited increasing genetic distance from the inoculum virus with time; (ii) clones obtained at a given time point branched out of the one immediately before, a clear demonstration of viral evolution; and (iii) clones from lymph nodes formed a cluster with those from plasma collected at the same time. In contrast, clones from treated animals, regardless of the tissue origin or time point, formed a cluster with clones derived from the plasma of the untreated animal at 8 wpi and the inoculum virus (Fig. 3; see Fig. S1). The results of the Highlighter plot analysis were consistent with those of the phylogenetic analysis. These results clearly demonstrated that viral evolution did not take place in SIV239-infected rhesus macaques during cART. Analysis of the *env* genes in the peripheral blood

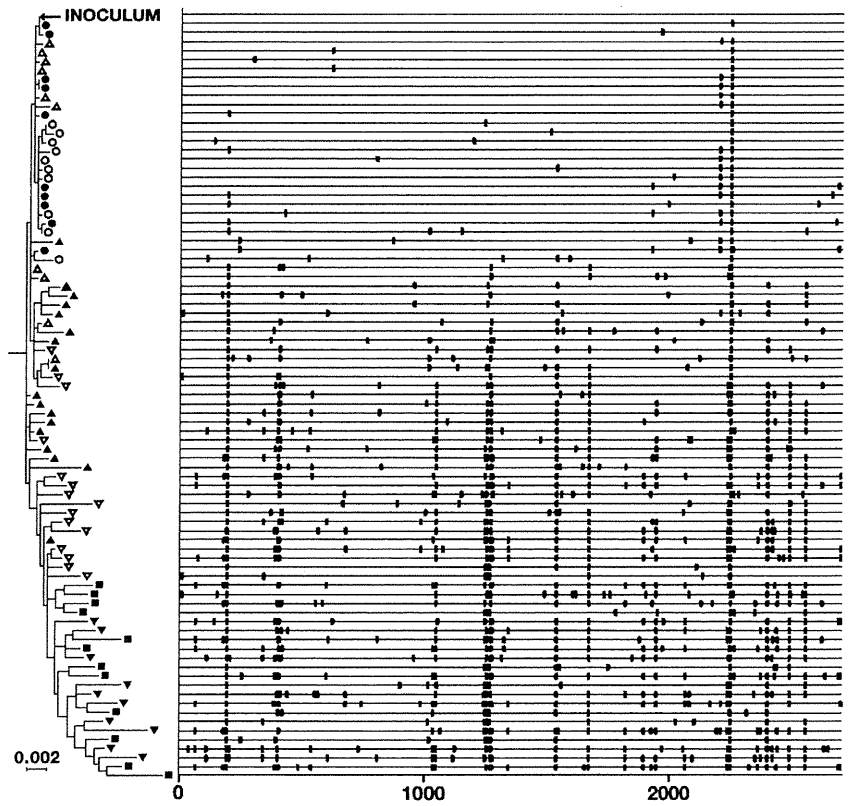

FIG 3 Phylogenetic relationship of *env* sequences from treated (MM530) and untreated (MM521) SIV-infected animals. Sequences of the entire *env* gene from both animals were subjected to phylogenetic analysis. The phylogenetic tree was constructed by the maximum-likelihood method (38). Open circles, sequences in the plasma of MM530 at 8 wpi; closed circles, those from the MLN of MM530 at 65 wpi; open triangles, those from plasma of MM521 at 8 wpi; closed triangles, those from plasma of MM521 at 18 wpi; open inverted triangles, those from plasma of MM521 at 42 wpi; closed inverted triangles, those from plasma of MM521 at 68 wpi; closed rectangles, those from MLN of MM521 at 68 wpi. The scale represents a genetic distance equivalent to 0.002 substitution/site. The corresponding sequence of SIVmac251 32H (GenBank accession no. D01065) was used as the outgroup.

mononuclear cells and gut-associated lymphatic tissues obtained from HIV-1 patients undergoing cART also found no evidence of *de novo* viral replication (13).

In contrast, other studies have reported continuous virus replication during combined chemotherapy (10, 12). One possible explanation for this discrepancy is the thorough suppression of the plasma viral burden, <20 copies/ml at necropsy, that was achieved in this study (18). *De novo* virus replication was detected in HIV-1-infected patients whose plasma viral RNA burdens ranged from 20 to 400 copies/ml but not in those with <20 copies/ml (24). Our findings also indicate that the cART regimen we used (18) was robust enough to halt viral evolution nearly completely in animals.

Our sample size, an average of 10 sequences from each specimen, may conceivably have limited our ability to detect minor populations with signs of ongoing replication. An analysis of four animals, however, did not reveal the genotypes detailed in the present study. Therefore, while our results cannot rule out possible *de novo* viral replication during cART, the data indicate that it is not a major mode of viral persistence in individuals whose virus replication levels are thoroughly suppressed by cART.

The locations of other potential viral reservoirs, in addition to resting $CD4^+$ T lymphocytes, an already established HIV/SIV reservoir found to be present in blood (25–28), lymph nodes (25), and the spleen (29), remains elusive. While the cART regimen we developed suppressed viral RNA levels nearly completely in the circulation and fairly well in effector sites, such as the gastrointestinal tract and lungs, viral RNA expression levels in lymph nodes were not contained effectively (18), suggesting that the viral reservoir consists of cells present in lymph nodes. We also detected CD3-positive cells, most likely $CD4^+$ T lymphocytes, expressing Nef protein in the follicles of the MLN of an SIV-infected animal that exhibited a viral rebound upon the cessation of cART (18). On the basis of their location, these might be Tfh cells, which are of the memory phenotype (30–32). The results of the present study have further narrowed the location of the viral reservoir from our previous study (18) to cells with longer half-lives that retain provirus for at least 1 year. Since resting $CD4^+$ T cells possess long half-lives (33), these cells satisfy this criterion for a viral reservoir during cART. It is conceivable that resting $CD4^+$ T cells functioned as the predominant viral reservoir in the SIV239-rhesus macaque model for patients undergoing cART employed in our study, as in preceding studies concerning the issue in the context of HIV and SIV infections.

Lymph nodes serve as a major HIV reservoir throughout the course of infection without intervention by cART (15–17). During clinical latency, the virus persists as an intact provirus, which can produce infectious viral particles upon cell activation, in a miniscule fraction of the resting $CD4^+$ T lymphocytes in lymph nodes (25). An extensive examination of lymph node specimens from HIV patients undergoing cART revealed an infinitesimal amount of viral RNA-positive cells by *in situ* hybridization (34). Hockett et al. (34) revealed that cART lowers the number of viral RNA-positive cells in lymph nodes but that the number of viral copies in each infected cell is constant, regardless of the viral burden in the circulation, suggesting the existence of virus-infected cells actively transcribing viral genes during cART, as we found previously in the lymph nodes of SIV239-infected animals undergoing cART (18). Our present observations, together with those of Hockett et al. (34), indicate that the viral RNA-positive cells present in lymph nodes during cART may represent cells infected with virus prior to the initiation of cART and transcribing viral RNA from integrated provirus during therapy.

Current cART is unable to eradicate the viral reservoir or, more precisely, provirus integrated in the reservoir. On the basis of our results, it is important to establish strategies to target specifically long-lived cells that harbor intact provirus while unlocking the dormant state of the provirus, perhaps by using histone deacetylase (35), to achieve a functional cure for AIDS.

ACKNOWLEDGMENTS

We are grateful to Tetsuro Matano for encouraging the initiation of this study, Beatrice H. Hahn for providing the protocol for SGA, and former and current members of the Igarashi laboratory for discussion and support.

This work was supported by Research on HIV/AIDS grants (H20-AIDS Research-003, H22-AIDS Research-007, and H24-AIDS Research-008) from The Ministry of Health, Labor and Welfare of Japan and by a Grant-in-Aid for Scientific Research (B) (23300156) from the Japan Society for the Promotion of Science.

REFERENCES

1. **Gulick RM, Mellors JW, Havlir D, Eron JJ, Gonzalez C, McMahon D, Richman DD, Valentine FT, Jonas L, Meibohm A, Emini EA, Chodakewitz JA.** 1997. Treatment with indinavir, zidovudine, and lamivudine in adults with human immunodeficiency virus infection and prior antiretroviral therapy. N. Engl. J. Med. 337:734–739.
2. **Hammer SM, Squires KE, Hughes MD, Grimes JM, Demeter LM, Currier JS, Eron JJ, Jr, Feinberg JE, Balfour HH, Jr, Deyton LR, Chodakewitz JA, Fischl MA.** 1997. A controlled trial of two nucleoside analogues plus indinavir in persons with human immunodeficiency virus infection and CD4 cell counts of 200 per cubic millimeter or less. AIDS Clinical Trials Group 320 Study Team. N. Engl. J. Med. 337:725–733.
3. **Perelson AS, Essunger P, Cao Y, Vesanen M, Hurley A, Saksela K, Markowitz M, Ho DD.** 1997. Decay characteristics of HIV-1-infected compartments during combination therapy. Nature 387:188–191.
4. **Quinn TC, Wawer MJ, Sewankambo N, Serwadda D, Li C, Wabwire-Mangen F, Meehan MO, Lutalo T, Gray RH.** 2000. Viral load and heterosexual transmission of human immunodeficiency virus type 1. Rakai Project Study Group. N. Engl. J. Med. 342:921–929.
5. **Autran B, Carcelain G, Li TS, Blanc C, Mathez D, Tubiana R, Katlama C, Debre P, Leibowitch J.** 1997. Positive effects of combined antiretroviral therapy on $CD4^+$ T cell homeostasis and function in advanced HIV disease. Science 277:112–116.
6. **Pakker NG, Notermans DW, de Boer RJ, Roos MT, de Wolf F, Hill A, Leonard JM, Danner SA, Miedema F, Schellekens PT.** 1998. Biphasic kinetics of peripheral blood T cells after triple combination therapy in HIV-1 infection: a composite of redistribution and proliferation. Nat. Med. 4:208–214.
7. **Zhang ZQ, Notermans DW, Sedgewick G, Cavert W, Wietgrefe S, Zupancic M, Gebhard K, Henry K, Boies L, Chen Z, Jenkins M, Mills R, McDade H, Goodwin C, Schuwirth CM, Danner SA, Haase AT.** 1998. Kinetics of $CD4^+$ T cell repopulation of lymphoid tissues after treatment of HIV-1 infection. Proc. Natl. Acad. Sci. U. S. A. 95:1154–1159.
8. **Antiretroviral Therapy Cohort Collaboration.** 2008. Life expectancy of individuals on combination antiretroviral therapy in high-income countries: a collaborative analysis of 14 cohort studies. Lancet 372:293–299.
9. **Chun TW, Davey RT, Jr, Engel D, Lane HC, Fauci AS.** 1999. Re-emergence of HIV after stopping therapy. Nature 401:874–875.
10. **Wong JK, Hezareh M, Günthard HF, Havlir DV, Ignacio CC, Spina CA, Richman DD.** 1997. Recovery of replication-competent HIV despite prolonged suppression of plasma viremia. Science 278:1291–1295.
11. **Shen L, Siliciano RF.** 2008. Viral reservoirs, residual viremia, and the potential of highly active antiretroviral therapy to eradicate HIV infection. J. Allergy Clin. Immunol. 122:22–28.
12. **Anderson JA, Archin NM, Ince W, Parker D, Wiegand A, Coffin JM, Kuruc J, Eron J, Swanstrom R, Margolis DM.** 2011. Clonal sequences recovered from plasma from patients with residual HIV-1 viremia and on intensified antiretroviral therapy are identical to replicating viral RNAs recovered from circulating resting $CD4^+$ T cells. J. Virol. 85:5220–5223.

13. Evering TH, Mehandru S, Racz P, Tenner-Racz K, Poles MA, Figueroa A, Mohri H, Markowitz M. 2012. Absence of HIV-1 evolution in the gut-associated lymphoid tissue from patients on combination antiviral therapy initiated during primary infection. PLoS Pathog. 8:e1002506. doi: 10.1371/journal.ppat.1002506.
14. Martínez MA, Cabana M, Ibanez A, Clotet B, Arno A, Ruiz L. 1999. Human immunodeficiency virus type 1 genetic evolution in patients with prolonged suppression of plasma viremia. Virology 256:180–187.
15. Embretson J, Zupancic M, Ribas JL, Burke A, Racz P, Tenner-Racz K, Haase AT. 1993. Massive covert infection of helper T lymphocytes and macrophages by HIV during the incubation period of AIDS. Nature 362: 359–362.
16. Pantaleo G, Graziosi C, Butini L, Pizzo PA, Schnittman SM, Kotler DP, Fauci AS. 1991. Lymphoid organs function as major reservoirs for human immunodeficiency virus. Proc. Natl. Acad. Sci. U. S. A. 88:9838–9842.
17. Pantaleo G, Graziosi C, Demarest JF, Butini L, Montroni M, Fox CH, Orenstein JM, Kotler DP, Fauci AS. 1993. HIV infection is active and progressive in lymphoid tissue during the clinically latent stage of disease. Nature 362:355–358.
18. Horiike M, Iwami S, Kodama M, Sato A, Watanabe Y, Yasui M, Ishida Y, Kobayashi T, Miura T, Igarashi T. 2012. Lymph nodes harbor viral reservoirs that cause rebound of plasma viremia in SIV-infected macaques upon cessation of combined antiretroviral therapy. Virology 423:107–118.
19. Leitner T, Albert J. 1999. The molecular clock of HIV-1 unveiled through analysis of a known transmission history. Proc. Natl. Acad. Sci. U. S. A. 96:10752–10757.
20. Shankarappa R, Margolick JB, Gange SJ, Rodrigo AG, Upchurch D, Farzadegan H, Gupta P, Rinaldo CR, Learn GH, He X, Huang XL, Mullins JI. 1999. Consistent viral evolutionary changes associated with the progression of human immunodeficiency virus type 1 infection. J. Virol. 73:10489–10502.
21. Burns DP, Desrosiers RC. 1991. Selection of genetic variants of simian immunodeficiency virus in persistently infected rhesus monkeys. J. Virol. 65:1843–1854.
22. Johnson PR, Hamm TE, Goldstein S, Kitov S, Hirsch VM. 1991. The genetic fate of molecularly cloned simian immunodeficiency virus in experimentally infected macaques. Virology 185:217–228.
23. Salazar-Gonzalez JF, Bailes E, Pham KT, Salazar MG, Guffey MB, Keele BF, Derdeyn CA, Farmer P, Hunter E, Allen S, Manigart O, Mulenga J, Anderson JA, Swanstrom R, Haynes BF, Athreya GS, Korber BT, Sharp PM, Shaw GM, Hahn BH. 2008. Deciphering human immunodeficiency virus type 1 transmission and early envelope diversification by single-genome amplification and sequencing. J. Virol. 82:3952–3970.
24. Günthard HF, Wong JK, Ignacio CC, Guatelli JC, Riggs NL, Havlir DV, Richman DD. 1998. Human immunodeficiency virus replication and genotypic resistance in blood and lymph nodes after a year of potent antiretroviral therapy. J. Virol. 72:2422–2428.
25. Chun TW, Carruth L, Finzi D, Shen X, DiGiuseppe JA, Taylor H, Hermankova M, Chadwick K, Margolick J, Quinn TC, Kuo YH, Brookmeyer R, Zeiger MA, Barditch-Crovo P, Siliciano RF. 1997. Quantification of latent tissue reservoirs and total body viral load in HIV-1 infection. Nature 387:183–188.
26. Chun TW, Finzi D, Margolick J, Chadwick K, Schwartz D, Siliciano RF. 1995. In vivo fate of HIV-1-infected T cells: quantitative analysis of the transition to stable latency. Nat. Med. 1:1284–1290.
27. Chun TW, Stuyver L, Mizell SB, Ehler LA, Mican JA, Baseler M, Lloyd AL, Nowak MA, Fauci AS. 1997. Presence of an inducible HIV-1 latent reservoir during highly active antiretroviral therapy. Proc. Natl. Acad. Sci. U. S. A. 94:13193–13197.
28. Finzi D, Hermankova M, Pierson T, Carruth LM, Buck C, Chaisson RE, Quinn TC, Chadwick K, Margolick J, Brookmeyer R, Gallant J, Markowitz M, Ho DD, Richman DD, Siliciano RF. 1997. Identification of a reservoir for HIV-1 in patients on highly active antiretroviral therapy. Science 278:1295–1300.
29. Shen A, Zink MC, Mankowski JL, Chadwick K, Margolick JB, Carruth LM, Li M, Clements JE, Siliciano RF. 2003. Resting CD4$^+$ T lymphocytes but not thymocytes provide a latent viral reservoir in a simian immunodeficiency virus-*Macaca nemestrina* model of human immunodeficiency virus type 1-infected patients on highly active antiretroviral therapy. J. Virol. 77:4938–4949.
30. Lindqvist M, van Lunzen J, Soghoian DZ, Kuhl BD, Ranasinghe S, Kranias G, Flanders MD, Cutler S, Yudanin N, Muller MI, Davis I, Farber D, Hartjen P, Haag F, Alter G, Schulze zur Wiesch J, Streeck H. 2012. Expansion of HIV-specific T follicular helper cells in chronic HIV infection. J. Clin. Invest. 122:3271–3280.
31. Lüthje K, Kallies A, Shimohakamada YT, Belz GT, Light A, Tarlinton DM, Nutt SL. 2012. The development and fate of follicular helper T cells defined by an IL-21 reporter mouse. Nat. Immunol. 13:491–498.
32. Weber JP, Fuhrmann F, Hutloff A. 2012. T-follicular helper cells survive as long-term memory cells. Eur. J. Immunol. 42:1981–1988.
33. Siliciano JD, Kajdas J, Finzi D, Quinn TC, Chadwick K, Margolick JB, Kovacs C, Gange SJ, Siliciano RF. 2003. Long-term follow-up studies confirm the stability of the latent reservoir for HIV-1 in resting CD4$^+$ T cells. Nat. Med. 9:727–728.
34. Hockett RD, Kilby JM, Derdeyn CA, Saag MS, Sillers M, Squires K, Chiz S, Nowak MA, Shaw GM, Bucy RP. 1999. Constant mean viral copy number per infected cell in tissues regardless of high, low, or undetectable plasma HIV RNA. J. Exp. Med. 189:1545–1554.
35. Archin NM, Liberty AL, Kashuba AD, Choudhary SK, Kuruc JD, Crooks AM, Parker DC, Anderson EM, Kearney MF, Strain MC, Richman DD, Hudgens MG, Bosch RJ, Coffin JM, Eron JJ, Hazuda DJ, Margolis DM. 2012. Administration of vorinostat disrupts HIV-1 latency in patients on antiretroviral therapy. Nature 487:482–485.
36. Tamura K, Nei M. 1993. Estimation of the number of nucleotide substitutions in the control region of mitochondrial DNA in humans and chimpanzees. Mol. Biol. Evol. 10:512–526.
37. Tamura K, Peterson D, Peterson N, Stecher G, Nei M, Kumar S. 2011. MEGA5: molecular evolutionary genetics analysis using maximum likelihood, evolutionary distance, and maximum parsimony methods. Mol. Biol. Evol. 28:2731–2739.
38. Felsenstein J. 1981. Evolutionary trees from DNA sequences: a maximum likelihood approach. J. Mol. Evol. 17:368–376.